OPTIMIZING VLHC SINGLE PARTICLE PERFORMANCE

Richard Talman

Laboratory of Nuclear Studies
Cornell University
Ithaca NY, 14853

ABSTRACT

Since the *sine qua non* of building the Very Large Hadron Collider (VLHC) is the ability to bend 50 TeV particles in a circle stably and cheaply, we concentrate on the "arcs" of the VLHC, excluding all other problems. Considering only single particle stability, the arcs are analysed using scaling considerations to choose the guide field B that minimizes cost. The extent to which the arcs can act as "achromatic optical fibers" for the beams is studied, in hopes of reducing the need for correction elements and spool pieces. Prescriptions are given to ameliorate the effects of resonance by choosing the best tunes and other parameters. If NbTi superconductor is used The optimal value for B seems to be about 3 Tesla, if NbTi superconductor is used.

1. Simplifying assumptions and guiding ideas

The strategy of this report is to concentrate on the tasks given in the abstract, especially that of selecting the optimal guide field B, while shamelessly ignoring all secondary complications. To permit introducing as minimal a set of quantities as possible, oversimplifications will be made, but they are supposed to be "neutral" with respect to describing the relative dependencies on magnetic field B. Only the arcs are considered, and they are taken to be perfectly repetitive. Designs and costs of straight sections, dispersion suppressors, intersection regions, *etc.* have to be obtained separately.

Synchroton radiation issues both good (damping) and bad (heating and anti-damping) will be ignored. So also will all current dependent problems. The magnets will be assumed to be superconducting (NbTi) but problems such as magnetization, hysteresis, persistent currents, and quench protection are ignored. Also the "new religion" will be adopted according to which random field quality is expected to be better than used to be assumed (say for the SSC). Field quality assumptions will be extrapolated from recent experience, mainly from the LHC.

As many "good ideas" as possible will be incorporated. Iron is expensive and stray fields are tolerable, therefore no iron. Return currents should be used to power the other ring. Multiple layer coils are unlikely to yield minimal cost. Since experience has shown that "most of the cost of magnets is in the ends" one should strive to eliminate ends, and that is done. Currents should flow in hollow (cooled) "transmission line-like" current carrying elements. Also spool pieces are expensive, so one should attempt to get rid of them.

Though I think most of these are, in fact, good ideas, the major purpose is to reduce the problem to its essentials, in order to provide a prescription for minimizing the total cost of magnet plus tunnel. The most important parameter to be chosen for the VLHC is its magnetic bend field B. Toward this end, in this paper all quantities will be expressed as functions of B only, and ultimately an optimal value for B will be determined, consistent with (admittedly uncertain) assumptions.

2. Lattice scaling relations

Accepting $E = pc = 50\,\mathrm{TeV}$ as the VLHC energy, the choice of B value implies a choice of average radius R,

$$R = \frac{pc/e}{cB} \quad \left(= 1.668 \times 10^5\, B^{-1} \right), \quad \text{or} \quad BR = 1.668 \times 10^5\,\text{T-m}. \tag{2.1}$$

(Where units are not given they are assumed to be M.K.S. Also numerical values will be quoted to unrealistically great precision to preserve their internal consistency.) We ignore the fact that the presence of straight sections will cause this to be in error by as much as 10%. Straight sections will have to be designed and paid for separately.

Another important lattice parameter to be chosen is the integer betatron tune Q. (Presumably $Q_x \approx Q_y$, but it will be shown that optimal tunes are separated by about 10%.) An elementary analysis by Chao[1] derives as a "law" the relation

$$Q = \zeta \sqrt{R} \quad \left(= 285.9\, B^{-1/2} \right). \tag{2.2}$$

(Chao is pleased to note that constant ζ is equal to $1\,\mathrm{m}^{-1/2}$ for all hadron and lepton accelerators, but the numerical value listed in Eq. (2.2) and all subsequent formulas result from a slightly different choice.) Chao offers "proof" of his law, but only for rings with bunch dimensions controlled by synchrotron radiation; for the VLHC generation of proton accelerators this proof is therefore only marginally applicable. Defining $\delta \equiv \Delta p/p$, if the r.m.s. energy spread σ_δ has its equilibrium value, Chao shows that scaling law Eq. (2.2) leads to the relation

$$\sigma_x = \sqrt{\epsilon_x \beta_x} \approx \eta \sigma_\delta, \tag{2.3}$$

where ϵ_x is horizontal emittance, β_x is horizontal beta function, and η is dispersion. In words this says that synchrotron and betatron oscillations place comparable demands on good field aperture. Below we will also show (barring dominant resonance) that this scaling causes the dynamic aperture due to chromatic correction to be the same for all accelerators. This inference (which neglects the incremental off-momentum aperture requirement) is consistent with the transverse dimensions of all accelerator vacuum chambers being the same. (This is true or false depending on ones standard of what passes for "equality".) Below, after inverting Eq. (2.3) to express σ_δ as a function of B, the neglected off-momentum aperture increment can be estimated.

More persuasive than these "proofs" is Chao's graph, shown in Fig. 2.1. I have taken the liberty of corrupting his law by plotting curves for both $\zeta = 1$ and $\zeta = 0.7$. There appears to be a tendency for proton accelerators to lie on the lower line and electron accelerators on the upper—some exceptions occur when proton and electron accelerators share tunnels, and hence tunes. The data suggests that the law is empirically valid even beyond the range of validity of its proof. Accepting this, I have plotted points for the proposed low field and high field VLHC options and have taken $\zeta = 0.7$ in the numerical version of Eq. (2.2).

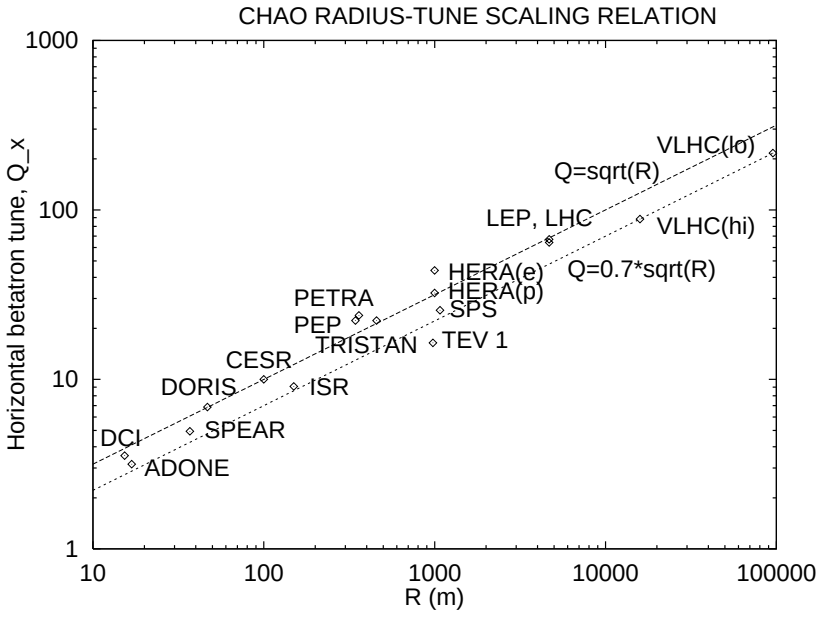

Figure 2.1: Relation between radius R and tune Q for existing high energy accelerators.

That $\mu_1 \approx \pi/2$ is (thought to be) optimal for the phase advance per cell can be inferred from the fact that both SSC and LHC designers made this choice. I adopt this value and treat the VLHC as made up of nothing but $\mu_1 \approx \pi/2$ regular cells. The number n of *half cells* is then given by

$$n = 8Q \quad \left(= 2287\, B^{-1/2} \right) . \tag{2.4}$$

and ℓ, the length per half cell is

$$\ell = \frac{2\pi R}{8Q} \quad \left(= 458.4\, B^{-1/2} \right) . \tag{2.5}$$

I continue by assuming pure FODO, thin lens cells, even though I will follow by arguing that combined function magnets are more economical. My purpose is to work with formulas that are simple, yet still reasonably accurate, especially as regards scaling dependence. It is not *a priori* obvious whether this choice is pessimistic or optimistic. Let $2q$ be the quad strength (*i.e.* inverse focal length) *per half cell* in such a lattice. The following formulas can then be derived:

$$\begin{aligned} q &= \frac{1}{\ell}\sin\frac{\mu_1}{2} \quad \left(= 1.543\times 10^{-3}\, B^{1/2}\,\mathrm{m}^{-1}\right), \\ \beta_{\max} &= \frac{1}{q}\sqrt{\frac{1+\ell q}{1-\ell q}}, \quad \beta_{\min} = \frac{1}{q}\sqrt{\frac{1-\ell q}{1+\ell q}}, \quad \frac{\beta_{\max}}{\beta_{\min}} \approx 5.8 \\ \beta_{\mathrm{typ}} &= \sqrt{\beta_{\min}\beta_{\max}} = \frac{1}{q} \quad \left(= 647.9\, B^{-1/2}\,\mathrm{m}\right), \\ \eta\,(s) &= \left(\frac{R}{Q^3}\right)^{1/2} \beta_x^{1/2}\,(s)\,, \\ \eta_{\mathrm{typ}} &\approx \frac{\eta_{\min}+\eta_{\max}}{2} \approx \frac{R}{Q^2} \quad (\,= 2.041\,\mathrm{m})\,. \end{aligned} \tag{2.6}$$

Note that the approximate relation between $\beta(s)$ and $\eta(s)$ is valid for all values of longitudinal position s. This makes Eq. (2.3) equally valid everywhere in the ring. Our value $\eta \approx 2\,\mathrm{m}$ differs from Chao's more pleasing result that typical dispersions are always 1 m because of our different choice of the factor ζ in Eq. (2.2). The sort of error we are tolerating can be estimated by comparing the value given for β_{typ} with another estimate;[†]

$$\beta_{\mathrm{ave}} = \frac{R}{Q} \quad \left(= 583.4\, B^{-1/2}\,\mathrm{m}\right). \tag{2.7}$$

The greatest demand for transverse acceptance occurs at the injection energy. To obtain absolute transverse particle displacements it is necessary to make assumptions concerning the transverse emittance and the injection energy. We arbitrarily assume $E_{inj} = 3\mathrm{TeV}$ which implies $\gamma_{inj} = 3197$. Taking $\epsilon_N = 3.75\times 10^{-6}$m-rad, which is the LHC value,[2] for

[†] Though β_{typ} and β_{ave}, being geometric mean of β's and $<1/\beta>^{-1}$ respectively, are different quantities, we regard these as two estimates, of "the same" quantity, that differ by 10%. There is an internal inconsistency of about the same amount in the formulas for η_{typ}. This should serve as warning that formulas in this paper are not to be adopted uncritically for accurate design. When numerical formulas are given to more significant figures than this it is only to retain internal consistency.

the normalized (one sigma) horizontal emittance, one obtains

$$\begin{aligned} \epsilon_x^{inj} &= \frac{\epsilon_N}{\gamma_{inj}} = 1.173 \times 10^{-9}\ \text{m-r}, \\ \sigma_{x,\max}^{inj} &= 1.355\, B^{-1/4}\text{mm}, \\ \sigma_\delta^{inj} &= \frac{\sigma_{x,\max}^{inj}}{\eta_{\max}} = 0.4056 \times 10^{-3}\, B^{-1/4}. \end{aligned} \tag{2.8}$$

Note that, even though these formulas refer to injection conditions, the factor B to be substituted is the full energy value—because B is just standing in proportionally for inverse radius R^{-1}.

In a bending magnetic field with nonuniform component $k_1 x + k_2 x^2/2 \sim qx + Sx^2/2$ (where q and S are "quad strength" and "sextupole strength" of the magnet) an off-momentum particle, because of its off-axis displacement $x = x_\beta + \eta\delta$, suffers excess angular displacement proportional to

$$\Delta x' \sim k_1 x_\beta\,(1-\delta) + \frac{1}{2} k_2 \left(x_\beta + \eta\delta\right)^2 + \cdots. \tag{2.9}$$

The magnet can be made "achromatic" by intentionally including sextupole field to cancel the momentum-dependent focusing terms proportional to $x_\beta\delta$;

$$k_2\,(s) = \frac{k_1\,(s)}{\eta\,(s)}. \tag{2.10}$$

Typically one compensates some chromaticity due to the intersection regions using the arc sextupoles but we ignore this complication. The unwanted side effect of the chromatic sextupoles is to reduce the dynamic aperture. On dimensional grounds (with resonant factors held constant) the dynamic aperature $x_{\rm da}$ satisfies

$$qx_{\rm da} \sim \frac{1}{2} S x_{\rm da}^2, \quad i.e. \quad x_{\rm da} = \text{ constant} \times \frac{q}{S} \approx 30\,\text{mm}, \tag{2.11}$$

where Eq. (2.10) and the last of Eqs. (2.6) have been used. The basis for this argument is that the aperture is some dimensionless factor times the amplitude at which nonlinear and linear forces are equal. The same scaling that holds η constant therefore holds $x_{\rm da}$ constant. The numerical estimate for $x_{\rm da}$ in Eq. (2.11) has been taken to match the LHC value.[3] (This is perhaps unjustifiably conservative since LHC lies well above the $\zeta = 0.7$ curve in Fig. 2.1.)

3. Magnet current distributions

Before continuing to estimate other lattice parameters we consider current configurations for superconducting magnets.

Elemental bend-like and quad-like current distributions are illustrated in Fig. 3.1. The magnetic fields they cause will be worked out to permit discussion of issues like field quality, current density, combined function designs and so on.

Bend-like currents: In terms of nominal magnet radius R_m and other parameters shown

$$\begin{aligned} &R_m = \sqrt{X^2+Y^2}, \quad a_1^2 = (X-x)^2 + Y^2, \quad a_2^2 = (X+x)^2 + Y^2, \\ &\cos\theta_1 = (X-x)/a_1, \quad \cos\theta_2 = (X+x)/a_2, \end{aligned} \tag{3.1}$$

the dependence on horizontal position x of the vertical component B_y of magnetic current is given by

$$\begin{aligned} B_y(x) &= 2\frac{\mu_0 I_d}{2\pi}\left(\frac{\cos\theta_1}{a_1} + \frac{\cos\theta_2}{a_2}\right) \\ &= \frac{2\mu_0 I_d}{\pi}\,\frac{X\left(X^2+Y^2\right) - Xx^2}{\left(X^2+Y^2\right)^2 + 2\left(-X^2+Y^2\right)x^2 + x^4} \\ &= \frac{2\mu_0 I_d}{\pi}\,\frac{X}{X^2+Y^2}\,\frac{1-\frac{1}{X^2+Y^2}\,x^2}{1+2\frac{-X^2+Y^2}{\left(X^2+Y^2\right)^2}\,x^2 + \frac{1}{\left(X^2+Y^2\right)^2}\,x^4}. \end{aligned} \tag{3.2}$$

Summing over all currents, the central field is

$$B = B_y(x)\,|_{x=0} = \frac{2\mu_0}{\pi}\sum_i \frac{X_i I_{d,i}}{X_i^2+Y_i^2} \approx \frac{\sqrt{3}\mu_0}{\pi}\,\frac{I_d}{R_m}, \text{ or } I_d \approx 1.443\times 10^6 R_m B, \tag{3.3}$$

where $I_d = \sum_i I_{d,i}$. The final estimate is based on assuming the dipole currents are "Helmholtz placed", $X_h = \sqrt{3}R_m/2$, $Y_h = R_m/2$. This choice cancels the sextupole coefficient of the sextupole part of the field, which is given by

$$k_2 = \frac{1}{BR}\,\frac{d^2B_y}{dx^2}\Big|_{x=0} = \frac{1}{BR}\,\frac{4\mu_0}{\pi}\sum_i \frac{X_i\left(X_i^2-3Y_i^2\right)}{\left(X_i^2+Y_i^2\right)^3} I_{d,i}, \tag{3.4}$$

where R must not be confused with R_m.

In Helmholtz configuration, to lowest approximation, B is unchanged by the distortion $X \to X+\Delta$, $Y \to Y-\Delta/\sqrt{3}$. This same deformation alters k_2;

$$\Delta k_2 \approx \frac{1}{BR}\,\frac{d^2B_y}{dx^2}\Big|_{x=0} = \frac{1}{BR}\,\frac{4\mu_0}{\pi}\frac{3\Delta}{R_m}\,\frac{I_d}{R_m^3} \approx \frac{1}{R}\,\frac{1}{R_m^2}\,4\sqrt{3}\,\frac{\Delta}{R_m}. \tag{3.5}$$

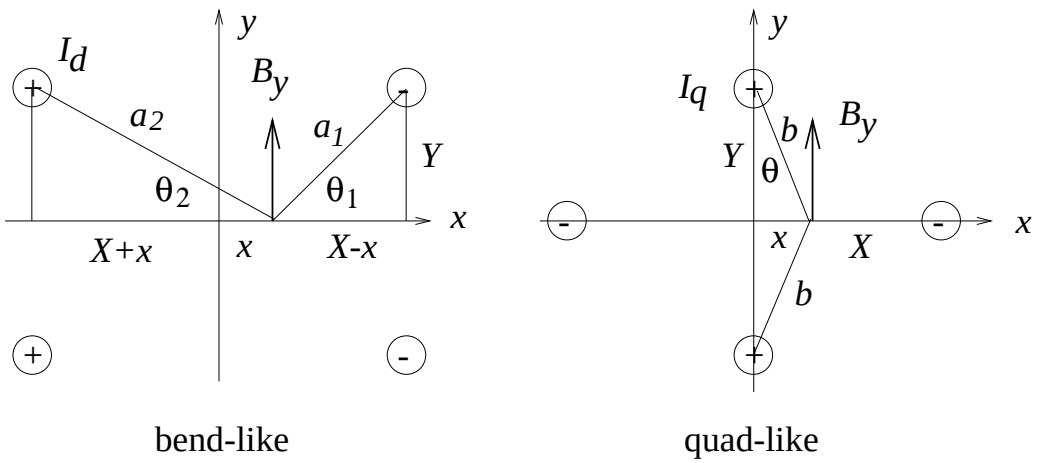

Figure 3.1: Elemental bend-like (even in x) and quad-like (odd in x) current distributions.

Quad-like currents: Defining $b^2 = Y^2 + x^2$, $\sin\theta = x/b$,

$$\begin{aligned} B_y(x) &= \frac{\mu_0 I_q}{2\pi}\left(\frac{1}{X-x} - \frac{1}{X+x} + \frac{2\sin\theta}{b}\right) \\ &= \frac{\mu_0 I_q}{\pi}\,\frac{X^2+Y^2}{X^2Y^2 + (X^2-Y^2)\,x^2 - x^4}\,x. \end{aligned} \tag{3.6}$$

The optical focusing coefficient k_1 is given by

$$k_1 = \frac{1}{BR}\,\frac{dB_y}{dx}\Big|_{x=0} = \frac{1}{BR}\,\frac{\mu_0 I_q}{\pi}\,\frac{X^2+Y^2}{X^2Y^2} \approx \frac{2}{\sqrt{3}}\,\frac{1}{RR_m}\,\frac{I_q}{I_d}. \tag{3.7}$$

The final estimate is based on assuming the quadrupole currents are optimally placed and the dipole currents are Helmholtz placed, $X_d = \sqrt{3}R_m/2$, $Y_d = R_m/2$, $X_q = Y_q = R_m$.

The three circuits shown in Fig. 3.1 can be adjusted to cancel the sextupole and decapole moments (with deformation $\Delta = 0$). The required currents are (in the ratios of) $I_{d1} = 0.1842\,\mathrm{A}$, $I_{d2} = 0.0909\,\mathrm{A}$, $I_{d3} = 0.0465\,\mathrm{A}$, yielding

$$B_y = \frac{\mu_0}{2\pi R_m}\left(1 - 0.267\left(\frac{x}{R_m}\right)^6 - 0.488\left(\frac{x}{R_m}\right)^8 + \cdots\right)\left(\frac{I_{d1}}{0.1842}\right). \tag{3.8}$$

For $R_m = 4\,\mathrm{cm}$, the leading multipole error is $-(0.267/4^6)x^6$ which can be quoted as 0.7 "units" (i.e. error in parts per 10^4 at 1 cm.) Because the required currents are so unequal, the conductor cross sectional area allotments shown in Fig. 3.1 are not at all optimal. But for purposes of rough estimate we invert Eq. (3.8) to give

$$I_{d1} \approx 0.921 \times 10^6 R_m\,B. \tag{3.9}$$

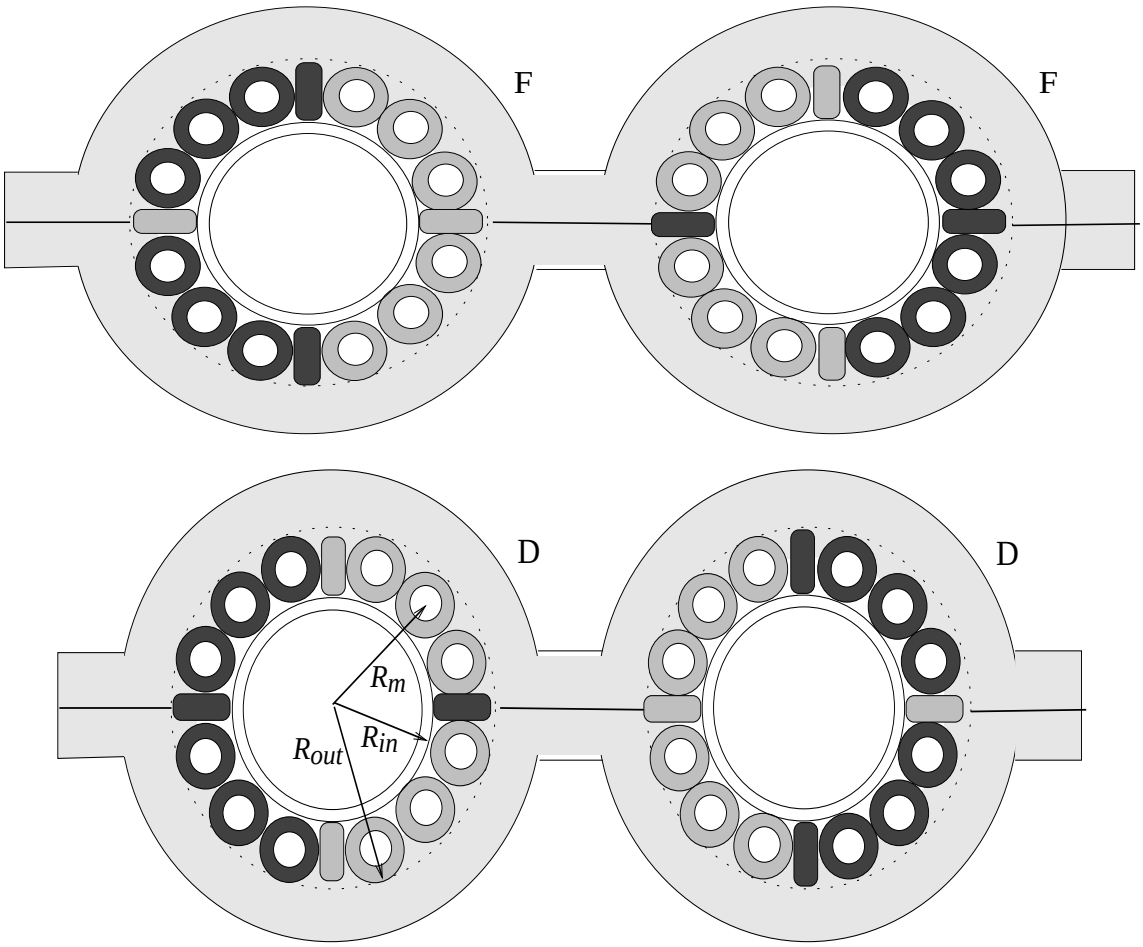

Figure 3.1: Suggested current distribution for ironless, "end-free", combined function VLHC magnets. There are three independent bend-like currents, I_{d1}, I_{d2}, I_{d3}, and one quad-like current I_q. The latter need to be "crossed" at the end of every half-cell. The F and D designations assume that "out" is to the right. The squashing and stretching required for chromatic compensation have been greatly exaggerated for visibility. Less than one percent deformation is actually required.

Since $\sum I_{d,i}$ evaluated from the individual currents listed here is roughly consistent with I_d as given by Eq. (3.3), for simplicity in the rest of this paper, the even more idealized Helmholtz configuration, with just one dipole current I_d, will be used.

4. Matching current distributions to lattice requirements

For optical properties, by ignoring the distinction between alternating gradient and thin lens FODO lattices we can combine magnet design formulas given above with the strength requirements imposed by the lattice. Remembering that q is the half-quad strength, and equating it to the length-strength product of the combined function dipole filling one half-cell, we obtain

$$k_1 = \frac{2q}{\ell} \ \left(= 0.6735 \times 10^{-5}\, B \right), \tag{4.1}$$

$$\frac{I_q}{I_d} = \frac{\sqrt{3}}{2}\, R R_m \frac{2q}{\ell} \ \left(= 5.833 \times 10^{-6} R_m\, RB = 5.833 \times 10^{-6} R_m \frac{pc/e}{c} = 0.972\, R_m \right). \tag{4.2}$$

I_q/I_d depends on B only implicitly through the magnet coil radius R_m and will be less than 10% (for $R_m < 0.1$ m as anticipated).

This ratio seems multiply surprising to me. Its smallness seems to make combined function design attractive for current-dominated magnets, because it avoids the expense of independent quadrupoles without using up much volume close to the beam for quadrupole current elements. Furthermore, because of the tendency for I_q/I_d to increase with increasing particle energy (because $R - m$ increases,) this argument would have been even more valid at lower energy. This makes it curious that existing proton rings have not adopted this design. In any case, Fig. 3.1 is intended to suggest the design for an ironless, combined function magnet, with appreciably less conductor allocated to quadrupole than to dipole currents. Such a magnet could be "end-free", with quadrupole leads twisting between half-cells but, otherwise, no need for electrical or coolant connections between half cells.

Ignoring "cross-talk" between magnets (present because no iron is present, but reducible to some extent by increasing separation) the three independent dipole currents and one quadrupole currents can be chosen to yield correct dipole, quadrupole, sextupole, and (zero) octupole field. This design seems to me to be more deserving of the name "cos-theta" than existing designs that go by that name. The fortuitous absence of octupole occurs because of the $X^2 - Y^2$ cancellation in the denominator of Eq. (3.6).

The design in Fig. 3.1 has another feature intended to overcome the fact that the configuration of currents that gives the desired chromatic correction in F cells will not compensate D cells correctly. The coils are squashed vertically and stretched horizontally

in F cells to give a positive sextupole coefficient, and the opposite is done in D sections. To estimate the deformation required for this we combine Eqs. (2.10), (3.5), and (4.1),

$$\frac{\Delta}{R_m} = \frac{1}{2\sqrt{3}}\, R_m^2\, \frac{1}{\eta\,(s)}\, \frac{2q}{\ell} \quad \left(\approx 0.0794\, R_m^2\, \frac{\eta_{\rm typ}}{\eta\,(s)} \right). \tag{4.3}$$

This tiny deformation has been greatly exaggerated in the figure, though it must be remembered that the local value $\eta(s)$ must be used; in vertically focusing section, $\eta(s)$ is approximately $0.5\eta_{\rm typ}$. Nevertheless the small value required for Δ/R_m makes it appear that there should be little extra cost to build chromatic correction into the dipole current distribution.

5. Current density requirements

According to Eq. (3.3) or (3.9), the required current I_d can be made arbitrarily small by choosing R_m small enough. Two considerations prevent going too far in this direction: need for vacuum chamber aperture and current density limitation. We now consider these limitations. So far the dipole current distribution has been idealized as line currents I_d flowing along the four Helmholtz lines. In fact the current flows over a region of area A such as is shown in Fig. 5.1. The angle $\Phi = 0.915\,\mathrm{r}$ has been chosen such that uniformly distributed current I_d yields the same central field as I_d flowing along the "Helmholtz line" at $(X_h, Y_h) = R_m(\sqrt{3}/2, 1/2)$. The coil quarter area is then

$$A = \frac{\Phi}{2}\left(R_{out}^2 - R_{in}^2\right), \quad \text{and} \quad I_d = J_{\rm eff}\, A = \xi\, J_c\, A, \tag{5.1}$$

where $J_{\rm eff}$ is the average current density, taken to be uniform over A and reduced from the critical current J_c by some derating factor ξ. The central field B is then still given by Eq. (3.3) provided that[†]

$$R_m = \frac{R_{out} + R_{in}}{2}. \tag{5.2}$$

According to the idealizations of the first section, we can take R_{in}, the inner coil radius, to be constant, independent of B. (Recall that this blames the chromatic sextupoles for the entire aperture requirement.) The SSC adopted the value $R_{in} = 20\,\mathrm{mm}$, and the VLHC should probably do the same, but for reasons to be explained below we will use the

[†] The formula for central field B remains valid even if $R_{out} >> R_{in}$, even though the formula "looks" approximate. But the current block shown in Fig. 5.1 does not necessarily cancel any nonlinear multipoles.

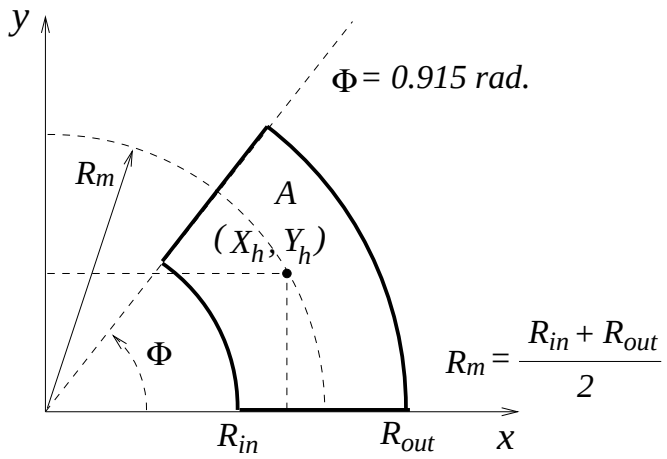

Figure 5.1: Effective conductor area A of one quadrant of a dipole magnet. The "Helmholtz" location is at $(X_h, Y_h) = R_m(\sqrt{3}/2, 1/2)$. R_{out} is adjustable but R_{in} is not (according to the idealizations of this paper.)

the LHC value[2], 28 mm. Then the field B can be increased only by increasing $J_{\rm eff}$ or by increasing the outer coil radius R_{out}. Combining Eqs. (3.3) and (5.1), we obtain

$$B = \frac{\sqrt{3}\mu_0}{\pi} J_{eff}\, \Phi\, (R_{out} - R_{in})\,. \tag{5.3}$$

The critical current density J_c for NbTi can be approximated as shown in Fig. 5.2,[4] by

$$J_{NbTi} \approx 10^{10}\, B^{-0.9}\, \mathrm{A/m^2}. \tag{5.4}$$

Above 6 Tesla this formula can be seen to overestimate J_{NbTi}. For simplicity in this paper we will still use Eq. (5.4) for all B, assuming, for example, that the operating temperature is reduced for large B to keep the formula correct. Then Eq. (5.3) can be solved for R_{out};

$$R_{out} = R_{in} + 1.577\times 10^6\, \frac{B}{J_{eff}} = R_{in} + \frac{1.577\times 10^{-4}\, B^{1.9}}{\xi}\, \frac{J_{NbTi}}{J_c}. \tag{5.5}$$

This dependence of R_{out} on B is plotted in Fig. 5.3 for various values of ξ. Fitting ξ to match the LHC value $R_{out} = 0.059\,\mathrm{m}$ yields $\xi = 0.285$. Choosing $\xi = 0.285$, the quarter coil area A (plotted in Fig. 5.4) is

$$A = \frac{0.915}{2}\left(\left(R_{in} + 5.53\times 10^{-4}\, B^{1.9}\, \frac{J_{NbTi}}{J_c}\right)^2 - R_{in}^2\right). \tag{5.6}$$

The strong dependence on B that has fueled the search for higher values of J_c to obtain higher magnetic field. The ratio $J_{\rm NbTi}/J_c$ has been left explicit to show how J_c must be

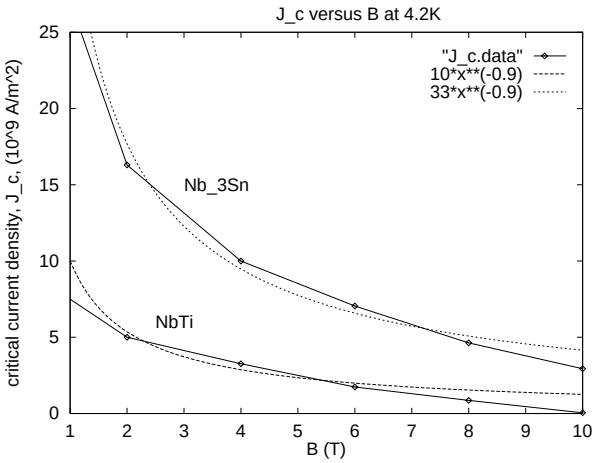

Figure 5.2: Critical current for NbTi and Nb_3Sn at 4.2K, over likely range for B.

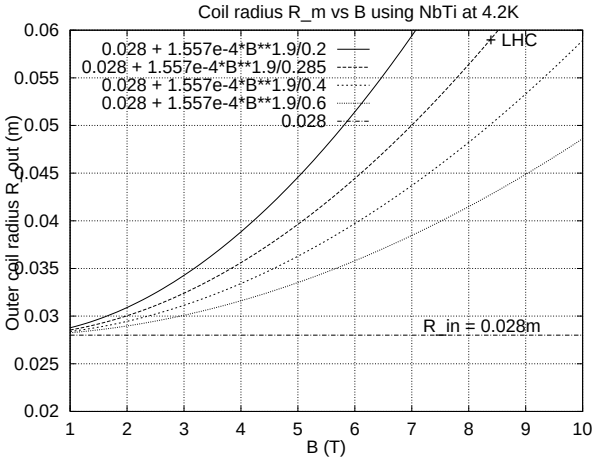

Figure 5.3: Outer coil radius R_{out} needed to produce central field B, using NbTi superconductor for $\xi = 0.2$, 0.285 (LHC value), 0.4, and 0.6 and with $R_{in} = 0.028$ m.

increased to hold magnet dimensions constant as B is increased. (The J_c improvement by a factor 3.3 in going from NbTi to Nb_3Sn at fixed temperature "buys" a factor $3.3^{1/1.9} = 1.87$ in B.)

The magnet can be further characterized by introducing the total energy content U of both channels. Since it is mainly the scaling behavior that will be used a rough approximate value should suffice. Taking the field volume (both rings) as $2(2\pi R)(2R_m)^2$, the energy

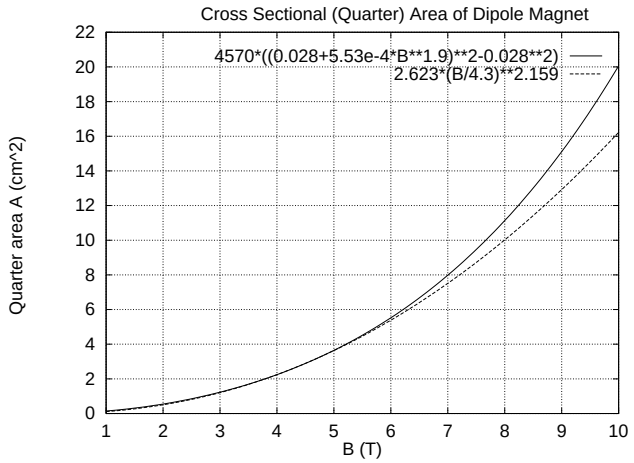

Figure 5.4: (Quarter) area A of dipole coil versus B. Also shown is a fit to the dependence $u \sim B^m$, yielding $m = 2.159$.

per meter u is given by

$$u = \frac{4}{\mu_0} B^2 R_m^2 f_{emp} \ , \tag{5.7}$$

where f_{emp} is an empirical factor to be matched to an existing magnet as in Table 5.1. u is plotted in Fig. 5.5.

Table 5.1: Empirical constant f_{emp} needed to match design report to $u = (4/\mu_0)B^2R_m^2f_{emp}$. These numbers should not be taken to be particularly reliable.

Accelerator	B T	R_{in} mm	R_{out} mm	R_m mm	u_{dr} MJ/m	u_{emp} MJ/m	f_{emp}
RHIC	4.3	40					
Tevatron	4.4	38.1	55.4	46.8	0.194×2	0.135	2.9
HERA(p)	4.72	≈ 37.5	≈ 58	≈ 47.7	0.162×2	0.161	2.0
SSC	6.6	20	40	30	0.0677×2	0.124	1.09
LHC	8.4	28	59	43.5	0.500	0.415	1.20

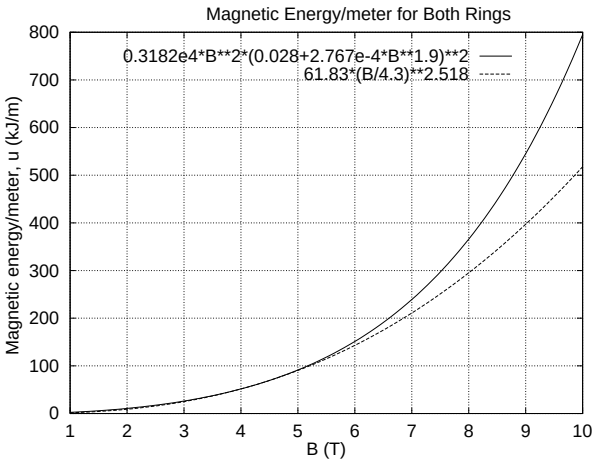

Figure 5.5: Stored energy per meter u (both rings), as given by Eq. (5.7) with $\xi = 0.285$ and $f = 1$. Also shown is a fit to the dependence $u \sim B^m$, yielding $m = 2.518$.

6. The storage ring as an optical fiber

Since light travels in straight lines one might suppose that an optical fiber would have to be perfectly straight for light to come out the other end. But of course this is wrong and moderate bending of the fiber causes no loss of intensity. One can hope that a storage ring will offer a similar benefit, with proton trajectories behaving like rays of light. This hope is well justified since, with gradient of index of refraction playing the role of focusing strength, in geometric optics approximation the equation satisfied by a confined ray in an optical fiber is the same as for a high energy particle in a focusing channel. Of course the gigantic difference in wavelength and the fact that optical fibers focus simultaneously in both transverse planes give optical fibers a huge advantage that may make the self-steering effect disappointingly small in a particle accelerator. For fiber optics the specification of tolerable "runout" can be quoted as a minimum bending radius or, more usefully, as its inverse, the maximum curvature. We now derive such a curvature limit for a storage limit, though we will express it as an "excess curvature" limit, since the ideal ring is itself curved. Expressed in this way the limit will apply equally to both horizontal and vertical motion.

Suppose the tangent to the nominal orbit is defined to be perfect at some arbitrary point taken to be the origin. The sagitta (*i.e.* transverse deviation from this tangent after arc length s) is given approximately by $0.5\, s^2/R$. From Eqs. (2.5), (2.2), and the last of

Eqs. (2.6),

$$\text{sagitta/cell } = 0.5 \left(\frac{4\pi R^{1/2}}{8\zeta}\right)^2 \frac{1}{R} = 2.52\,\text{m}, \tag{6.1}$$

which is approximately the same as the typical dispersion, η_{typ}—another remarkable "universal constant" for all accelerators.

Because of this systematic horizontal sagitta accumulation it is less confusing to concentrate on vertical curvature, and to find the degree to which self-steering allows the ring to deviate from a single plane, assuming the orbit plane and lattice plane coincide at the origin. Let us define σ_δ/R to be the "tolerable excess curvature" or "one sigma excess curvature" since a particle that is off-momentum by "one sigma" can be said to suffer a tolerable deviation from the central orbit. The maximum deviation from the initial plane will occur if this excess persists for one quarter of a full revolution.†

$$\text{maximum vertical deviation from equiplanarity } = 0.5 \left(\frac{\pi R}{2}\right)^2 \frac{\sigma_\delta}{R} = 83.4\, B^{-5/4}\,\text{m}. \tag{6.2}$$

Several meters of runout, either horizontal or vertical, over one quarter of the ring is therefore tolerable. In principle, this permits the ring to "terrain follow" even with no steering elements. This is a pleasant result, though the allowable runout is perhaps not large enough obviate the need for steering elements; but very few should suffice. Since the allowable deviation increases quadratically with circumferential distance the tolerable runout over shorter distances is much less. For example,

$$\text{maximum vertical deviation after } N \text{ cells } = 0.5\,(2N\ell)^2 \frac{\sigma_\delta}{R} = 1.02\, N^2\, B^{-1/4}\,\text{mm}. \tag{6.3}$$

In an optical fiber the dependence of index of refraction on radial coordinate is far from linear. This suggests that the importance of nonlinearity in accelerators may have been over-emphasized in the past. The main factor that discourages this hope is that particles make multiple passes of the lattice which subjects the storage ring to resonant degradation. However there is an adiabatic condition which, if satisfied, presumably assures emittance preservation over a single passage. This condition is that the fractional change in betatron

† If the excess curvature persists for half a revolution then the nomimal plane of the lattice could have been chosen to reduce the maximum deviation. The deviation calculated in Eq. (6.2) visualizes a "roller coaster shape" raised at both ends.

wavelength be small compared to 1 over a circumferential distance equal to one betatron wavelength (which is $2\pi\beta_{\rm ave}$).

7. Minimizing total cost of arcs

Wishing to convert all parameters to definite numbers, we must pick a value for magnetic field B, presumably by minimizing the cost. Even restricting discussion to the arcs of the VLHC (treated as one continuous circle) since one has only unreliable cost figures, minimizing its cost requires a certain amount of guess work. The model to be employed is that the cost is the sum of two parts, a "tunnel plus cryostat part" C_T, proportional to circumference and hence scaling as B^{-1}, and a "magnet part" C_M that scales as B^m where m is a positive power.

Estimated costs of the tunnel alone by Willen[5] are in the range $\$1000 - \$3000$/m and, glancing at cost breakdown for RHIC, one can guess that the cryostat cost is perhaps \$3000/m. Assuming that much of this cost is associated with end effects and the (now declared to be unnecessary) spool pieces, we take $c_T = \$4000$/m as the portion of VLHC arc cost that scales as B^{-1}.

According to Gourlay[6] the cost of procuring superconducting wire represents an appreciable fraction (perhaps one third) of the magnet cost for existing accelerators, For our "end-free, iron-free" magnet this material cost will represent an even larger fraction. According to Fig. 5.4 this cost per meter should scale proportional to B^m with $m = 2.2$. This dependence may be too weak since, using Gourlay's numbers for LHC and RHIC, the conductor mass-per-meter scaling exponent is $m = 2.7$. According to Fig. 5.5 the scaling of stored energy per meter (often a good indicator of cost) is more extreme ($m = 2.8$) and some costs undoubtedly scale much less steeply.† Table 5.1 shows that our empirical formula for magnetic energy does not match existing machines very well; this may be due to their appreciably different values of R_{in}.

Again referring (uncritically) to costs reported by Willen, the cost of RHIC 4.3 Tesla magnet was about $c_M = \$10,000$/m. To convert this into a VLHC cost one hopes to reduce this by more than a factor of two due to the "absence of ends", much smaller bore size, and

† For some reason magnet costs are frequently quoted as cost per Tesla-meter, but I see no justification whatsoever for this, especially since it leads to the optimal field being infinite.

other economies of design and fabrication, but must increase it by a factor of 1.8 for two-in-one design. Assume then that the cost per meter is in the range $c_{M,ref} = \$5 - 10K/\mathrm{m}$ at $B_{ref} = 4.3\,\mathrm{T}$.

To incorporate the dependence on B let $c_M = c'_M B^m$. With R given by Eq. (2.1), the separate costs and their sum are

$$\begin{aligned} C_T &= c_T\, 2\pi R \quad \left(= 1.048 \times 10^6\, c_T\, B^{-1} \right), \\ C_M &= c'_M B^m\, 2\pi R \quad \left(= 2.362 \times 10^4\, c_{M,ref}\, B^{1.6} \right), \\ C &= C_T + C_M = \mathrm{const}_T\, B^{-1} + \mathrm{const}_M\, B^{m-1} \end{aligned} \tag{7.1}$$

Varying B to minimize C yields

$$B_{\mathrm{opt}} = \left(\frac{c_T}{(m-1)\, c'_M} \right)^{1/m}, \quad \frac{C_M}{C_T} = \frac{1}{m-1}. \tag{7.2}$$

This shows that, after optimization, if $m > 2$ as expected, the tunnel costs more than the magnet, independent of c_M and c_T.

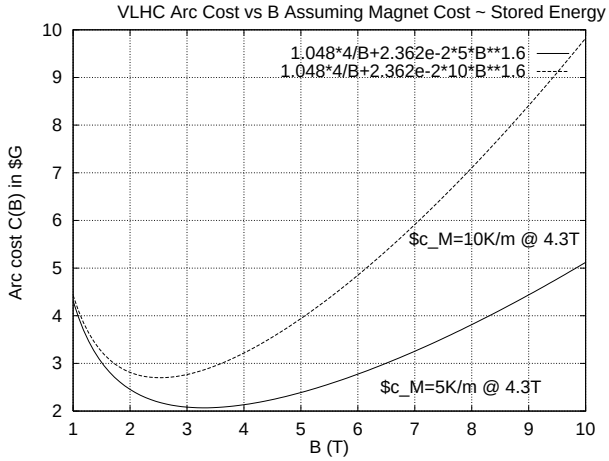

Figure 7.1: Arc cost $C_T + C_M$ (tunnel and magnet) in billions of dollars assuming magnet cost is proportional to stored magnetic energy.

8. Choice of Tunes

Since there is no strong dependence of aperture on B or E, the aperture degradation due to magnetic field nonlinearity should be similarly insensitive. This means that tunes that are optimal for the VLHC can be obtained by applying prescriptions that yield optimal tunes for the LHC. I have written two reports on this subject.[7] In these papers a figure of merit FOM is defined which is a fractional reduction in acceptance at an "intermediate" amplitude, such as 10 sigma. That is, a physical scraper set to scrape at 10 sigma assuming linear optics would actually scrape at $10(1 - FOM)$ sigma. Being at intermediate amplitudes this distortion is analytically calculable. The analytic expression for FOM has numerator and denominator factors that are both sensitive to resonance. They can be independently analysed and optimized.

100*FOM = percentage acceptance reduction at 10 sigma due to randoms

qy =	0.270	0.278	0.286	0.294	0.302	0.310	0.318	0.326	0.334	0.342	0.350
qx=											
0.260	11.5	9.5	8.8	8.5	8.6	8.9	9.7	11.1	34.4	12.4	13.6
0.264	14.3	10.1	9.0	8.7	8.7	9.0	10.0	11.3	34.7	12.8	14.5
0.268	28.9	11.3	9.5	8.9	8.9	9.2	10.6	11.5	35.0	13.3	15.6
0.272	28.9	14.3	10.2	9.3	9.1	9.4	xxxx	11.8	35.4	14.0	17.0
0.276	14.3	29.0	11.5	9.8	9.4	9.6	11.1	12.1	35.9	14.8	18.9
0.280	11.4	29.0	14.5	10.6	9.9	10.0	11.0	12.5	36.4	15.7	21.6
0.284	10.2	14.4	29.3	12.0	10.5	10.4	11.2	13.0	37.1	17.0	25.5
0.288	9.6	11.6	29.4	15.1	11.3	10.9	11.6	13.6	37.9	18.5	32.1
0.292	9.2	10.5	14.9	29.9	12.8	11.6	12.1	14.3	38.8	20.6	45.0
0.296	9.1	10.0	12.2	30.1	16.0	12.6	12.8	15.3	40.0	23.5	83.3
0.300	9.0	9.7	11.1	15.7	30.9	14.2	13.8	16.7	41.5	27.7	xxxx

The denominator factor of FOM is maximized by choosing fractional tunes that "stay away from low order resonances", and for this it is the fractional tunes that are important. The best compromise is found by making a fine grain scan of FOM in the vicinity of tunes that have been found empirically to be favorable. It is mainly random field errors that influence this optimum. There are probably numerous comparably good regions of the tune plane, but in any region the optimum tune is well-defined. The table above shows a scan of one such region, $0.26 < Q_x < 0.30$, $0.27 < Q_y < 0.35$, assuming field errors anticipated for the LHC. Other than narrow resonances, marked xxxx, and $Q_x = Q_y$ and $Q_y = 1/3$ bands, the region of good tunes is about ± 0.02 for both planes. Most early tracking studies for the LHC were performed at $Q_x = 0.28$, $Q_y = 0.31$ which was found to

be satisfactory. Further tracking studies showed that the aperture was somewhat better at the values $Q_x = 0.26$, $Q_y = 0.30$ shown to be optimal in the table, but the difference between $FOM = 0.085$ and $FOM = 0.10$ is not great.

The analytic formula for the numerator factor of FOM can be expressed as a phasor sum over nonlinearities present in the lattice. It is mainly systematic field errors that influence this optimum. For phase advance per cell near 90°, the dominant nonlinear elements (other than chromatic sextupoles) are octupoles, both skew and erect. The reason for this is that the phase advance per cell is multiplied by either 4 or 0, to obtain the phasor angle, so systematic octupole errors tend to accumulate coherently. Fig. 8.1 shows FOM calculated on a grid of of integer tunes centered on nominal SSC integer tunes, 60, 60. Again there are many resonances, each contributing additively to an overall FOM value. In the figure each of these contributions is displayed as a circle with radius proportional to the contribution to FOM. The tune choice with the smallest maximum contribution therefore has the smallest surrounding circle. That is, $Q_x = 65,\ Q_y = 58$, the choice I will adopt, though there are other comparably good choices. Tracking studies for the LHC have shown that this choice is superior to the previously nominal tunes of $Q_x = 63,\ Q_y = 59$.[8] However the somewhat less split choice $Q_x = 64,\ Q_y = 59$ (which is also a good choice according to Fig. 8.1 has been tentatively adopted. According to theoretical arguments due to Verdier[9] there is an even more favorable choice $Q_x = 68,\ Q_y = 59$, and this also appears to be confirmed by tracking. But there may be engineering or cost reasons that make such a large split unjustified. Based on these considerations, in the following table, the integer tunes are chosen approximately as $0.95 < Q >$ and $1.05 < Q >$. Of course the integer tunes will have to be shifted up somewhat when intersection regions and other straight sections are included, but the fractional tunes will stay the same.

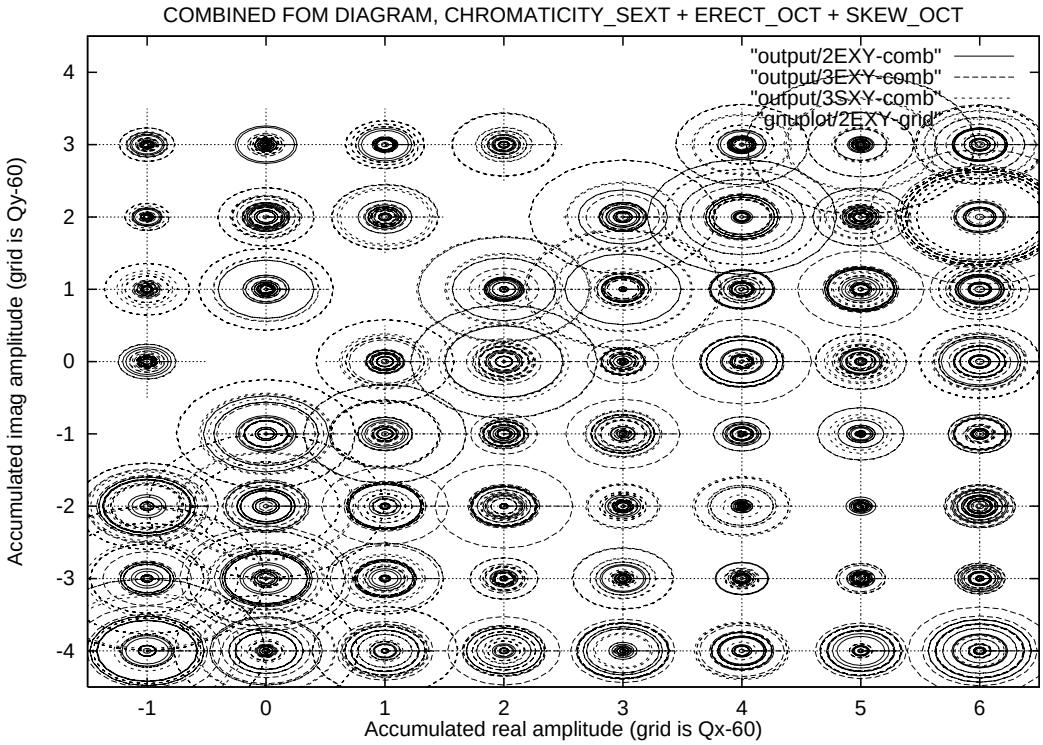

Figure 8.1: FOM values with chromaticity sextupoles plus erect octupole plus skew octupole, all superimposed. The optimal integer tunes are clearly $Q_x = 65$, $Q_y = 58$.

9. References

1. A. Chao, *Elementary Design and Scaling Considerations of Storage Ring Colliders*, SLAC and Fermilab Summer Schools, AIP 153, 1987.
2. The LHC Study Group, *The Large Hadron Collider*, CERN/AC/95-05, 1995.
3. J.-P. Koutchouk, *The LHC Dynamic Aperture*, PAC conference proceedings, New York, 1999.
4. M.W. Wilson, *Superconducting Materials for Magnets*, CERN Accelerator School on Superconductivity in Particle Acclerators, CERN 96-03.
5. Erich Willen, *Superconducting magnets*, INFN Eloisatron Project 34'th Workshop, Erice, Sicily, 1996, and BNL 64183.
6. S. Gourlay, *Magnet Cost Issues*, VLHC Magnet Workshop, 1998.
7. R. Talman, *Tune Optimization for Maximum Dynamic Acceptance, I: Formulation*, LHC Project Report 197, July, 1998. R. Talman, *Tune Optimization for Maximum Dynamic Acceptance, II:*$Q_x = 65$, $Q_y = 58$, LHC Project Report 233, August, 1998.
8. J-P. Koutchouk, *The LHC Dynamic Aperture,* PAC conference proceedings, Vancouver, 1998.
9. A. Verdier, *Resonance Free Lattices for AG Machines*, PAC conference proceedings, Vancouver, 1998. F. Schmidt and A. Verdier, *Optimization of the LHC Dynamic Aperture via the Phase Advance of the Arc Cells*, PAC conference proceedings, Vancouver, 1998.

Table 8.1: VLHC PARAMETERS ($c_M = \$5\,\mathrm{K/m}$)

Parameter		units	Low field	Minimum cost	High field
B	field	Tesla	1.8	3.3	12
R	radius	km	92.7	50.5	13.9
$< Q >_{int}$	mean (int) tune		213	157	82
Q_x			224.26	165.26	86.26
Q_y			202.30	149.30	78.30
ell	half-cell length	m	341.6	252.3	132.3
q	half-quad str.	1/m	0.002071	0.002804	0.005345
β_{max}		m	1166	861.4	451.7
β_{typ}		m	483.1	356.8	187.1
η_{max}		m	3.342	3.342	3.342
$\sigma^{inj}_{x,max}$		mm	1.170	1.005	0.7279
σ^{inj}_{δ}		per/mil	0.3500	0.3008	0.2178
Id	dipole current	kA	74.93	146.0	1023
Iq	quad current	kA	2.102	4.355	58.74
R_{in}	min coil radius	mm	28	28	28
R_{out}	max coil radius	mm	29.69	33.35	90.15
R_m	mean coil radius	mm	28.85	30.67	59.07
A	coil 1/4 area	cm^2	0.447	1.502	33.62
u	stored energy/m	kJ/m	8.582	32.58	1599
"optical fiber"	max runout	m	40.0	18.8	3.74
	runout/cell	mm	0.88	0.76	0.55
C_T	tunnel cost	\$G	2.329	1.270	0.3492
C_M	magnet cost	\$G	0.3251	0.8159	5.790
C	total cost	\$G	2.654	2.086	6.139